Bioorganic & Medicinal Chemistry Letters 18 (2008) 4368–4372

Contents lists available at ScienceDirect

Bioorganic & Medicinal Chemistry Letters

journal homepage: www.elsevier.com/locate/bmcl

Exploring 9-benzyl purines as inhibitors of glutamate racemase (MurI) in Gram-positive bacteria

Bolin Geng [a,*], Gloria Breault [a], Janelle Comita-Prevoir [a], Randy Petrichko [a], Charles Eyermann [a], Tomas Lundqvist [b], Peter Doig [a], Elise Gorseth [a], Brian Noonan [a]

[a] AstraZeneca R&D Boston, Infection Discovery, 35 Gatehouse Drive, Waltham, MA 02451, USA
[b] AstraZeneca R&D Mölndal, Global Structural Chemistry, Mölndal, SE-43183, Sweden

ARTICLE INFO

Article history:
Received 30 April 2008
Revised 18 June 2008
Accepted 19 June 2008
Available online 24 June 2008

Keywords:
Glutamate racemase
MurI inhibitor
Benzyl purine

ABSTRACT

An early SAR study of a screening hit series has generated a series of 9-benzyl purines as inhibitors of bacterial glutamate racemase (MurI) with micromolar enzyme potency and improved physical properties. X-ray co-crystal EI structures were obtained.

There has been a growing need for new antibacterials to fight resistance, especially antibacterials with novel mechanism of action (MOA) to combat 'bad bugs' such as MRSA and VRE.[1,2] A research program was initiated to develop a Gram-positive antibacterial agent through inhibition of glutamate racemase (MurI), an essential enzyme involved in bacterial peptidoglycan biosynthesis (Scheme 1).[3–5] The *murI* gene is conserved in all bacterial species that synthesize peptidoglycan, and its essentiality has been demonstrated in several bacterial species. In the literature, substrate mimetic inhibitors have been designed.[6] The rationale for us to target this particular spectrum (*Staphylococcus aureus, Enterococcus faecalis, Enterococcus faecium*, etc.) was based on the high degree of MurI sequence identity and biochemical similarity in these selected Gram-positive pathogens. Phylogenic analyses demonstrate that the MurI from Gram-positive bacteria cluster to a single clade.[7] High-throughput screening (HTS) of the AstraZeneca compound collection identified several hit series with low micromolar potency against *E. faecalis* MurI. A 9-benzyl purine scaffold was selected as one series to be advanced to the Lead Identification phase. Here, we describe our Hit-to-Lead effort (Fig. 1).

Based on the biological profile of the hits such as compound **1**, our objectives during the Lead Identification phase were to increase MurI enzyme inhibitory potency, improve physical properties, especially solubility, and to expand the Gram-positive spectrum. Our strategy to achieve these goals was to systematically vary substituents on position 2, 6, and 9 of the purine scaffold, followed by purine core modification.

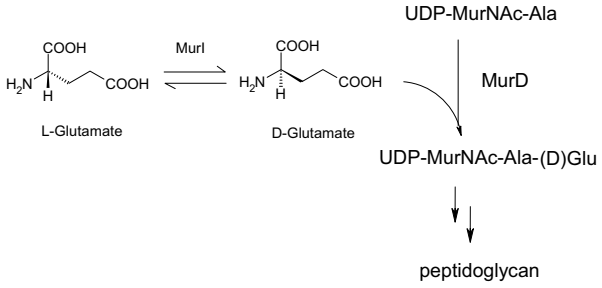

Scheme 1. The role of glutamate racemase (MurI) in the peptidoglycan precursor biosynthetic pathway.

The synthesis of 9-benzyl-2-butylthio purines of type **I**, listed in Table 1, as shown in Scheme 2, was readily achieved by benzyla-

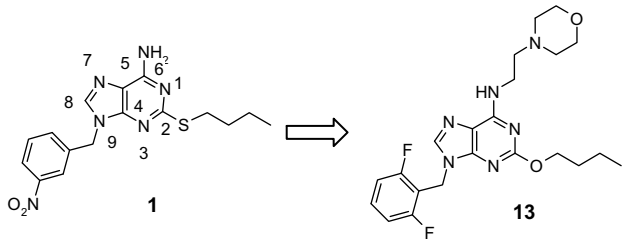

Figure 1. Representative HTS hit compound **1** and lead compound **13**.

* Corresponding author. Tel.: +1 781 839 4297; fax: +1 781 839 4230.
E-mail address: bolin.geng@astrazeneca.com (B. Geng).

0960-894X/$ - see front matter © 2008 Elsevier Ltd. All rights reserved.
doi:10.1016/j.bmcl.2008.06.068

Table 1
R9 Benzyl variations (Type **I**, R6 = H)

n	R9	R2–Q	*E.fa*[a,b] (μM)	*E.fm*[a,b] (μM)	*S.au*[a,b,c] (μM)	Solu. (μM)
1	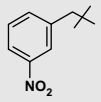	*n*-Bu-S	9.4	17.7	>400	42
2	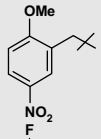	*n*-Bu-S	1.4	2.5	>400	25
3	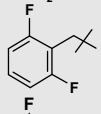	*n*-Bu–S	4.1	6.0	>400	50
4	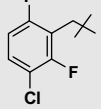	*n*-Bu-S	2.2	2.6	>400	25
5	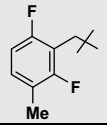	*n*-Bu-S	5.4	6.5	>400	25

[a] *E.fa*, *Enterococcus faecalis*; *E.fm*, *Enterococcus faecium*; *S.au*, *Staphylococcus aureus*; solu., solubility (nephelometry).
[b] Activity against MurI isozymes from several bacterial species was assessed by IC_{50} determination for assay protocol see Ref. 7.
[c] Four hundred micromolar is the highest no-effect concentration tested. Same in Tables 2–4 where 400 μM was used.

tion of a 2-butylthio-purine intermediate.[8,10] This 2-butylthio-purine intermediate was obtained through the following sequence: treatment of 4,6-diamino pyrimidine-2-thiol with sodium hydroxide in methanol was followed by solvent evaporation and the resultant solid was reacted with 1-bromobutane in DMF. Introduction of the nitroso group was achieved using sodium nitrite in water. Subsequent catalytic hydrogenation gave the 4,5,6-triamine intermediate, which was cyclized by refluxing the triamine in formamide.

To diversify substitution on positions 2 and 6, a route using aromatic displacement 6-Cl of 2,6-dichloro purine, followed by N-alkylation, then second displacement of 2-Cl with R2-QH reagents (Q=O, alcohols; Q=NH, amines) was employed as shown in Scheme 3.[9] The order of steps b and c can be switched to ease the purification. Using this sequence the compounds of type **II** listed in Tables 2 and 3 were obtained.

Four purine core modifications were performed as shown in Schemes 4–7. Alkylation of commercially available purinyl-2-thiol followed by benzylation gave the 6-des amino derivatives (type **III**).[10] The purin-6-one analogs (type **IV**) were easily accessed by diazotation–hydrolysis through the Sandmeyer reaction.[11] The triazolopyrimidine (*aza*-purine) derivatives (type **V**) were prepared

Table 2
R2-Q chain variations (Type **II**, R6 = H)

n	R9	R2–Q	*E.fa* (μM)	*E.fm* (μM)	*S.au* (μM)	Solu. (μM)
5	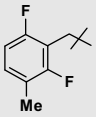	*n*-Bu-S	5. 4	6. 5	>400	25
6	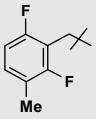	*n*-Bu-O	9.8	27	>400	50
7	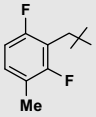	1-(C_2F_5)–*n*-Pr-O	4. 3	4.4	>400	25
8	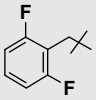	*n*-Bu-NH	26.1	42.5	>400	100
9	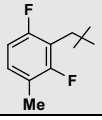	1-(AcNH)-Et-O	167	>400	>400	100

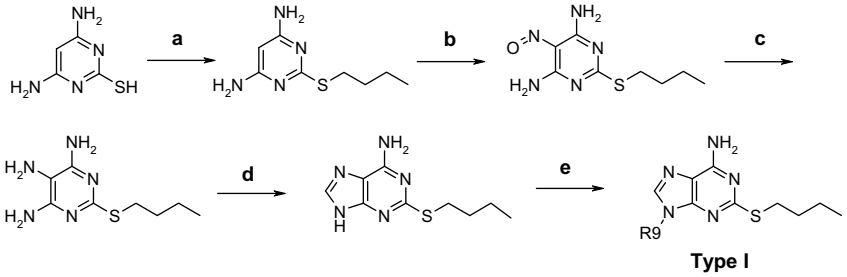

Scheme 2. General synthesis of 2-butylthio purines. Reagents and conditions: (a) NaOH, Methanol, *n*-BuBr, DMF; (b) $NaNO_2$, water; (c) H_2, PtO_2, Ethanol; (d) $HCONH_2$, reflux; (e) BnBr or other R9 electrophiles, Cs_2CO_3, DMF.

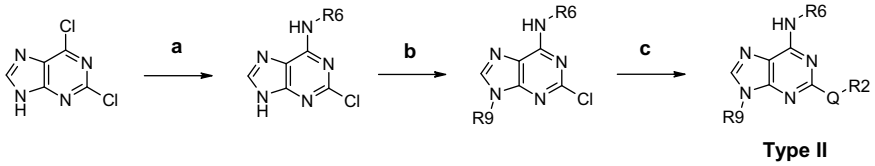

Scheme 3. General synthetic route. Reagents and conditions: (a) ammonia or $R6NH_2$, methanol; (b) BnBr or other R9 electrophiles, Cs_2CO_3, DMF; (c) butanol, NaOH, reflux.

Table 3
R6 variations (Type **II**, R2–Q = *n*-Bu-O)

n	R9	R6	*E.fa* (μM)	*E.fm* (μM)	*S.au* (μM)	Solu. (μM)
6	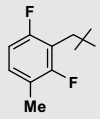	H	9.8	27	>400	50
10	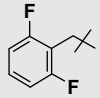	Methyl	5.5	13.9	>400	100
11	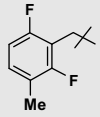	Benzyl	>400	>400	>400	3.1
12	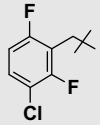	Pyridin-3-ylmethyl	2.0	2.7	>400	18
13	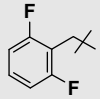	2-(4-Morpholino)ethyl	5.8	5.5	>400	200

by reacting the product 4,5,6-triamine from step c in Scheme 2[12] with sodium nitrite. The 8-purinone analogs (type **VI**) were prepared by hydrolysis of the corresponding 8-methoxy intermediate according to literature.[13]

Data shown in Table 1 revealed the trend that ortho substituents on the benzyl ring tended to increase potency. However, variations of the substituent on the benzyl ring afforded, in general, no significant potency improvements against *E.fa* and *E.fm* MurI enzyme and no inhibition of the *S.au* enzyme activity was observed. Further benzyl replacement analogs containing small alkyl, bicyclic heterocycles, and benzoyl substituents during an SAR expansion study resulted in reduction of activity (data not shown). The fact that the SAR at the 9-position is relatively unresponsive and that only lipophilic groups were tolerated, meant that it would be difficult to obtain substantial improvements in physical properties from modifications at this position. In subsequent rounds of optimization, the 2,6-difluoro substituents on benzyl moiety at R9 were kept constant while more polar solubilizing groups were introduced at R2-Q on the 2-position of the molecule to reduce lipophilicity of the molecule (Table 2). It was gratifying to discover that the simple S to O switch of linking atom Q at 2-position (compound **6**) not only retained the enzyme potency, but also gained a twofold increase in solubility. Further optimization along this direction did not yield potency improvement. Polar groups were not tolerated as exemplified in compound **9**. Here the introduction of the acetamide at the end of the R2 chain resulted in more than 15-fold potency loss in *E.fa* MurI inhibitory activity and the compound became completely inactive against *E.fm* MurI. An O to NH switch (compound **8**) was attempted based on the expectation of additional solubility increases, but again this resulted in potency losses. Further SAR expansion using branched alkyls, cyclic alkyls, benzyls, and aromatics generated only compounds with reduced activity (data not shown). Oxidizing the linking atom sulfur to sulfone destroyed inhibitory activity. These data suggest that enzyme potency for linkage Q follows the order: $S \sim O > NH \gg SO_2$. We concluded that linear 4–5 carbon chains provided ideal shape, size, and lipophilicity at R2 position and hypothesized that, similarly to R9, hydrophobic residues must surround the R2 region in the enzyme-binding pocket.

The SAR of the 6-position was in sharp contrast to the 2- and 9-position. Solubilizing groups were well tolerated. There is a striking difference between benzylamino (compound **11**) and pyridin-3-ylmethyl amino (compound **12**) analogs as shown in Table 3. The former compound was completely inactive and the latter was among one of the most potent inhibitors of both *E.fa* and *E.fm* MurI. An exciting example was the 2-(4-morpholino)ethyl amine group (compound **13**), as it not only retained all potency against both *E.fa* and *E.fm* MurI enzymes, but also delivered a substantial boost in solubility (equilibrium solubility 99 μM). This improved solubility allowed us to obtain an X-ray co-crystal structure using *E.fa* MurI. This structure (1.65 Å) provided a working rationale for understanding the potency discrepancy among MurI isozymes studied, and laid the foundation for the project to potentially advance to full Lead Optimization phase.

The inhibitor compound **13**[14] binds at each of two cryptic symmetrical allosteric hydrophobic pockets on the MurI homodimer

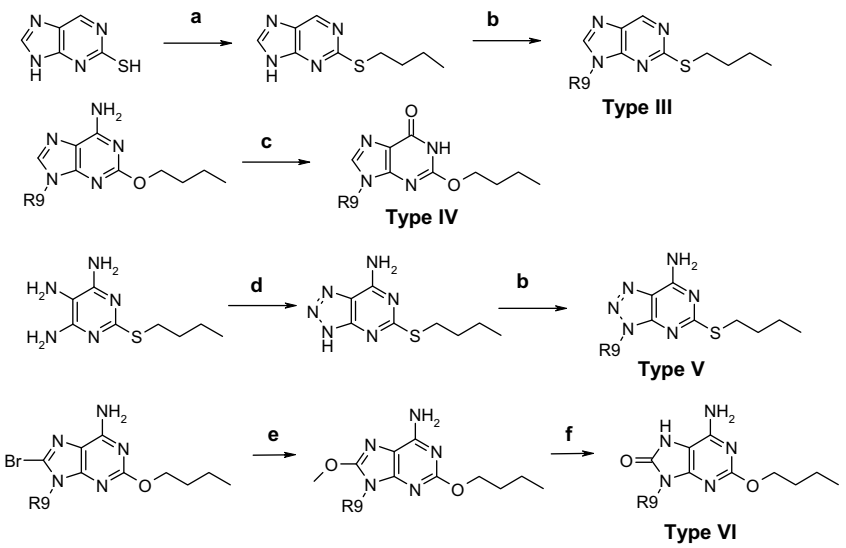

Schemes 4–7. Purine core modifications. Reagents and conditions: (a) *n*-BuBr, Et_3N, DMF; (b) BnBr or other R9 electrophiles, Cs_2CO_3, DMF; (c) $NaNO_2$, H_2O; (d) $NaNO_2$, Ethanol; (e) NaOMe, Methanol; (f) HCl.

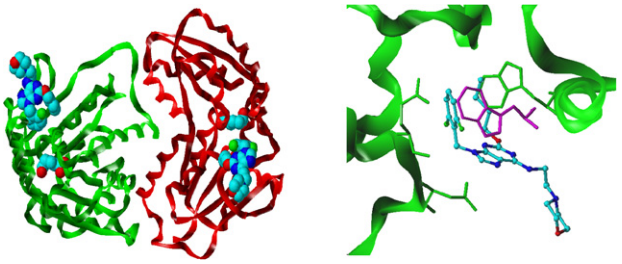

Picture 1. (Left) Compound **13** binds at each of two allosteric sites of *E. faecalis* MurI dimer. (Right) Detailed view at one allosteric binding pocket. C-terminal Trp 254 was displaced. Magenta shows the original position of Trp 254 in apo MurI. Asn 155 (below purine core) and Glu 153 (close to benzyl ring) were also shown.

Table 4
Core modifications (Type **III**–**VI**)

n	Core structure	*E.fa* (μM)	E.fm (μM)	*S.au* (μM)	Solu. (μM)
14	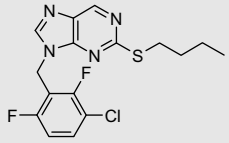	1. 0	1. 8	>400	50
15	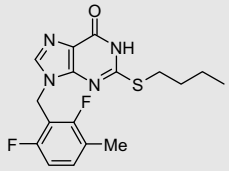	11.5	3.75	>400	100
16	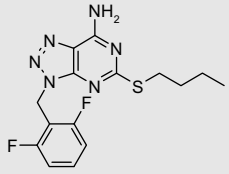	4. 3	6. 2	>400	50
17	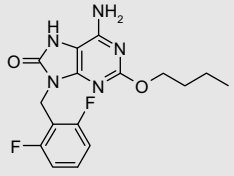	38.1	97.8	>400	200

(Picture 1). There seems to be a 'hydrophobic collapse',[15] a term often used in protein folding, between R2 and R9 to pre-organize these two groups in the binding conformation (Picture 1, left and right). Upon formation of the pocket, the R2 carbon chain displaced the Trp254 indole ring out of original location and formed π hydrophobic interactions. In subsequent attempts to explore this hydrophobic region, we observed that double bonds on the R2 chain were tolerated, consistent with improved π stacking interactions with Trp254. As we expected, R9 benzyl interacts with hydrophobic side chains of Val14, Ile190, and Ile 250. One edge of the benzyl group is solvent exposed and could be appropriately substituted to improve interaction with Glu153. The region corresponding to R6 substituent pocket is close to the solvent front, which explained its tolerance of polar groups and its intolerance of lipophilic substituents. Morpholino group is indeed positioned toward solvent and is not forming significant interactions with the enzyme. A tentative rationale for the striking *E.fa* and *S.au* isozyme potency profile differences was proposed based on this co-crystal structure. By comparing the binding pocket residues of apo enzyme of *S.au* and above co-crystal structure of *E.fa*, it was observed that a key amino acid at the binding site Asn155 present in the *Enterococcus* MurI protein was replaced with Met153 in *S.au*. The Asn155 provides weak polar interaction with purine core while Met153 certainly does not.

Modification to the purine core gave varied results (Table 4). The des-amino compound **14** showed an increase in enzyme potency, while Type **VI** compound 8-Purinone **17**[13] was less active. Compounds such as type **IV** 6-purinone **15** and type **V** triazolopyrimidine (aza-purine) derivative **16** did not resulted in significant change in enzyme potency. Similar to the profiles observed in the type **I** and type **II** scaffolds, all of these four core-modification analogs still had the same spectrum issue. Finally, all of the MurI inhibitors described in this Letter exhibit relatively weak antibacterial activity (some compounds show MIC of 16–64 μg/ml, data not shown) against selected Gram-positive pathogens.

From our perspective, these compounds represent viable lead series for further optimization, particularly given the potential for enzyme:inhibitor structure-enabled scaffold design[17] to increase intrinsic potency and continued improvement of physical properties. Issues to address in further optimization cycles include antibacterial potency and desired antibacterial spectrum,[16] as well as improvement in physical properties. In this regard, the type **II** analogs with a handle at 6-position may provide further optimizing flexibility, especially for physical property improvement to reduce plasma protein binding (PPB) and to enhance cell penetration.

In conclusion, we discovered a novel series of MurI inhibitors against selected Gram-positive MurI isozymes, which have the potential to be further optimized into an anti-Gram positive bacteria agent.

Acknowledgment

The authors thank Microbiology Department at AstraZeneca R&D Boston for MIC determination.

References and notes

1. Bush, K. *Clin. Microbiol. Infect.* **2004**, *10*, 10.
2. Payne, D. J.; Gwynnn, M. N.; Holmes, D. J.; Rosenberg, M. *Methods Mol. Biol.* **2004**, *266*, 231.
3. (a) Doublet, P.; van Heijenoort, J.; Mengin-Lecreulx, D. *J. Bacteriol.* **1992**, *174*, 5772; (b) Glavas, S.; Tanner, M. E. *Biochemistry* **2001**, *40*, 6199.
4. Doublet, P.; van Heijenoort, J.; Mengin-Lecreulx, D. *Biochemistry* **1994**, *33*, 5285.
5. Van Heijenoort, J. *Nat. Prod. Rep.* **2001**, *18*, 503.
6. For competitive inhibitors: (a) Glavas, S.; Tanner, M. E. *Bioorg. Med. Chem. Lett* **1997**, *7*, 2265; (b) Tanner, M. E.; Miao, S. *Tetrahedron Lett.* **1994**, *35*, 4073; (c) De Dios, A.; Priesto, L.; Martin, J. A.; Rubio, A.; Ezquerra, J.; Tebbe, M.; Lopez de Uralde, B.; Martin, J.; Sanchez, A.; LeTourneau, D.; McGee, J. E.; Boylan, C.; Parr, T. R., Jr.; Smith, M. C. *J. Med. Chem.* **2002**, *45*, 4559; For peptide ligand, see: (d) Kim, W. C.; Rhee, H. I.; Park, B. K.; Suk, K. H.; Cha, S. H. *J. Biomol. Screen.* **2000**, *5*, 435.
7. For investigation of structural and regulatory diversity of glutamate racemases, see: Lundqvist, T.; Fisher, S. L.; Kern, G.; Folmer, R. H. A.; Xue, Y.; Newton, D. T.; Keating, T. A.; Alm, R.; de Jonge, B. L. M. *Nature* **2007**, *447*, 817.
8. (a) Laxer, A.; Major, D. T.; Gottlieb, H. E.; Fischer, B. . *J. Org. Chem.* **2001**, *66*, 5463; (b) Temple, D. L. Jr.; US patent 4286093, 1981.; (c) Benedich, A.; Tinker, J. F.; Brown, G. B. *J. Am. Chem. Soc.* **1948**, *70*, 3109.
9. (a) Komatsu, H.; Araki, T. *Nucleosides, Nucleotides and Nucleic Acids* **2005**, *24*, 1127; (b) Kurimoto, A.; Ogita, H. JP2005089334 A, Jpn. Kokai Tokkyo Koho, 2005.
10. Kikugawa, K.; Suehiro, H.; Aoki, A. *Chem. Pharm. Bull.* **1977**, *25*, 1811.
11. Kelley, J. L.; Schaeffer, H. J. *J. Heterocycl. Chem.* **1986**, *23*, 271.
12. Roblin, R. O., Jr.; Lampen, J. O.; English, J. P.; Cole, Q. P.; Vaughan, J. R., Jr. *J. Am. Chem. Soc.* **1945**, *67*, 290.
13. Kurimoto, A.; Ogino, T.; Ichii, S.; Isobe, Y.; Tobe, M.; Ogita, H.; Takaku, H.; Sajiki, H.; Hirota, K.; Kawakami, H. *Bioorg. Med. Chem.* **2004**, *12*, 1091.
14. Beside compound **13**, additional three X-ray co-crystal structures including compound **12** were obtained and same binding mode was observed. Interestingly, a small molecule X-ray crystal structure for compound **12** (data not shown), also shows a similar 'hydrophobic collapse' of R2 and R9 that we observed in E–I co-crystal structures. All compounds were purified by recrystallization, silica gel chromatograph or preparative Gilson HPLC

depending on initial purity of final step synthesis and characterized by LC-MS and NMR techniques.*Analyticals of compound* **13**: MS (ES^+): 447 (MH^+) for $C_{22}H_{28}F_2N_6O_2$ ^{1}H NMR (DMSO-d_6) δ: 1.00 (t, 3H); 1.48 (m, 2H); 1.72 (m, 2H); 2.60 (m, 4H); 3.64 (m, 6H); 4.27 (t, 2H); 5.43 (s, 2H); 7.21 (t, 2H); 7.54 (m, 1H); 7.64 (br s, 1H); 8.05 (s, 1H).

15. For hydrophobic collaps, see: Rich, D. H. *Perspect. Med. Chem.* **1993**, 15.
16. For a recent review on challenges of target-based antibacterial discovery, see: Payne, D. J.; Gwynn, M. N.; Holmes, D. J.; Pompliano, D. L. *Nat. Rev. Drug Discov.* **2007**, *6*, 29.
17. AutoDep EBI-36519 PDB ID code **2vvt** for the coordinate entry.